Macalester Journal of Physics and Astronomy

Volume 9
Issue 1 *Spring 2021*

Article 6

May 2021

Model of Electromagnetic Waves in an Axion-Induced Parity Symmetry Violation

Sarah Lipstone
Macalester College, slipston@macalester.edu

Model of Electromagnetic Waves in an Axion-Induced Parity Symmetry Violation

Abstract

Axion particles have been postulated to resolve the strong CP problem in Quantum chromodynamics. The axion field may double as the inflaton field that produces cosmic inflation. In this project, we use a combination of analytical and numerical analysis to study how axion-induced parity symmetry violation affects the dynamics of electromagnetic waves.

Cover Page Footnote

Prof. Tonnis ter Veldhuis advised me on this project.

Model of Electromagnetic Waves in an Axion-Induced Parity Symmetry Violation

Sarah Lipstone *

5 April 2021

Abstract

Axion particles have been postulated to resolve the strong CP problem in Quantum chromodynamics. The axion field may double as the inflaton field that produces cosmic inflation. In this project, we use a combination of analytical and numerical analysis to study how axion-induced parity symmetry violation affects the dynamics of electromagnetic waves.

1 Background

1.1 Parity

Parity is a property that a pair of objects can have. One of the best examples for describing parity is a pair of hands. A person's hands typically look the same and have similar properties; however, because they are mirror images of each other, they are not exactly the same – if a person places the palm of their hand on the back of their other hand, it is clear that their hands are not the same. This concept can be applied to waves. Two waves, one right-handed and the other left-handed, can have similar scalar properties and thus be

*Professor Tonnis ter Veldhuis advised me on this project.

mirror images of each other – when this happens, it is said that these waves exhibit parity. In comparison, if the velocity of one of those waves were changed, then those two waves would exhibit parity violation. For this project, the axion field will cause parity violation in the electromagnetic waves.

1.2 Maxwell's Equations

Maxwell's equations (Equations (1)-(4)) are at the core of this project because they define the basic properties of electromagnetic waves and describe how they are propagated. To simplify future calculations, it is assumed that they have no source and are linear. Furthermore, they do not exhibit parity violation because Maxwell's equations alone do not account for the factors that cause parity violation.

$$\vec{\nabla} \cdot \vec{E} = 0 \tag{1}$$

$$\vec{\nabla} \cdot \vec{B} = 0 \tag{2}$$

$$\vec{\nabla} \times \vec{E} = -\frac{\partial \vec{B}}{\partial t} \tag{3}$$

$$\vec{\nabla} \times \vec{B} = \frac{1}{c^2}\frac{\partial \vec{E}}{\partial t} \tag{4}$$

1.3 Lagrangian Density

The Lagrangian density, shown in Equation (5), is a mathematical summary of the field and is needed to study the properties of generalized waves. The field tensors (Equation (6)) contain the electromagnetic field, and the axion field, represented by φ, is incorporated with the coupling constant, h. While this axion field has not actually been measured in nature, the axion particles are a proposed solution to the strong CP problem in quantum

chromodynamics and are a valid mathematical solution for the cause of parity violation; thus, they are included in the model for this project.

$$\mathcal{L} = -\frac{1}{4}F_{\mu\nu}\eta^{\mu\alpha}\eta^{\nu\beta}F_{\alpha\beta} - \frac{1}{2}\partial_\mu\varphi\eta^{\mu\nu}\partial_\nu\varphi - \frac{1}{2}m^2\varphi^2 + h\varphi\varepsilon^{\mu\nu\alpha\beta}F_{\mu\nu}F_{\alpha\beta} \tag{5}$$

$$F_{\mu\nu} = \begin{bmatrix} 0 & -\frac{E_x}{c} & -\frac{E_y}{c} & -\frac{E_z}{c} \\ \frac{E_x}{c} & 0 & B_z & -B_y \\ \frac{E_y}{c} & -B_z & 0 & B_x \\ \frac{E_z}{c} & B_y & -B_x & 0 \end{bmatrix} \qquad F^{\mu\nu} = \begin{bmatrix} 0 & \frac{E_x}{c} & \frac{E_y}{c} & \frac{E_z}{c} \\ -\frac{E_x}{c} & 0 & B_z & -B_y \\ -\frac{E_y}{c} & -B_z & 0 & B_x \\ -\frac{E_z}{c} & B_y & -B_x & 0- \end{bmatrix} \tag{6}$$

As a result, the first term in Equation (5) contain Maxwell's equations, and the rest of the terms couple the axion field, represented by φ, with the electromagnetic field. When φ is uniform and constant with respect to time, the electromagnetic waves exhibit parity – however, when φ is no longer uniform, parity is violated. From this density, the equations used in the computational models to simulate the electromagnetic and axion fields are derived.

2 Methods and Implementation

The following equations are derived from Equation (5) and are the foundation of the simulation.

$$\frac{\partial^2\varphi}{\partial n^2} - \vec{\nabla}^2\varphi + m^2\varphi + 4h\vec{E}\cdot\vec{B} = 0 \tag{7}$$

$$-\frac{\partial \vec{E}}{\partial n} + \vec{\nabla} \times \vec{B} + 4h\frac{\partial \varphi}{\partial n}\vec{B} + 4h\vec{\nabla}\varphi \times \vec{E} = 0 \tag{8}$$

$$\frac{\partial \vec{B}}{\partial n} + \nabla \times \vec{E} = 0 \tag{9}$$

If these equations were implemented as they were, there would be multiple issues that would prevent Mathematica from even attempting the calculation. First, these equations are analytical. To compute $\vec{E}$, $\vec{B}$ and φ, the computer needs somewhere to start and somewhere to end – since these equations are coupled, there is no clear initial point to begin the computation and no clear end point. Second, these equations to not explicitly define for the computer what makes up the components of the $\vec{E}$, $\vec{B}$ and φ. While this might be clear to a person studying the equations, it is not clear to the computer. Finally, the equations do not explicitly state what the boundary conditions are.

2.1 Finite Difference Time Domain

To determine the boundary conditions, the finite difference time domain (FDTD) model, also known as Yee's method, is used. In this model, it is assumed that space-time can be describe by discrete points – for the case of this project, the electric and magnetic fields can be modeled by discrete points in a field. Furthermore, the FDTD model assumes that all points of the electric and magnetic fields depend on the difference of the previous points. The only exception is that the initial points of the electric and magnetic fields are determined by the initial conditions of the electromagnetic wave. [1]

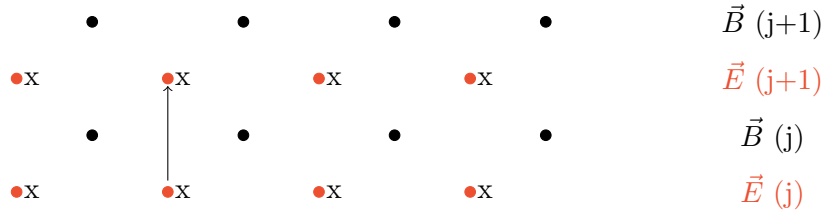

Figure 1: Staggered Lattice Model

2.2 Staggered Lattice

Building on the FDTD model, the staggered lattice model, shown in Figure 1, is also implemented. In this model, there are alternating rows of components of $\vec{E}$ and $\vec{B}$ in terms of i and j index values, and the φ field is represented by the x's. The i index represents the position index and increases from left to right, and the j index represents the time index and increases from the bottom. The points of the rows are staggered with respect to the neighboring rows. As a result, this model provides a clear solution for which points are needed to calculate updated values.

For example, consider the problem of finding $E_x(i, j+1)$ from $E_x(i, j)$ as illustrated by the arrow in Figure 1. In addition to $E_x(i, j)$, the points from the surrounding B and φ fields are needed for the calculation. When looking at the model, it is expected that the two B field points, $B_x(i, j)$ and $B_x(i+1, j)$, are needed because they are directly to the left and right, respectively, of the line. Additionally, it is expected that $\varphi(i, j)$, $\varphi(i-1, j)$, $\varphi(i+1, j)$, $\varphi(i, j+1)$, $\varphi(i-1, j+1)$, and $\varphi(i+1, j+1)$ are needed because they too surround the arrow visualizing the update of $E_x(i, j)$ to $E_x(i, j+1)$.

2.3 Update Equations

Equations (10)-(14) are used in all cases to update $\vec{E}$, $\vec{B}$ and φ. Equation (10) is derived from Equation (7), Equations (11) and (12) are derived from Equation (8), and Equa-

tions (13) and (14) are derived from Equation (9). The indices in these update equations were determined by the staggered lattice, as described in the above example. In all these equations, there are five common constants needed for the computational aspect of the program, all of which are dimensionless. Nz is the total number of time-steps, Nn is the total number of space-steps, dz is the change in each time-step, dn is the change in each space-step, m is the mass, and h is the coupling constant, which is used to combine the electromagnetic and φ fields.

$$\begin{aligned}\varphi(i,j+2) =& dn^2\Bigg[-\frac{1}{dn^2}[-2\varphi(i,j+1)+\varphi(i,j)]-m^2\varphi(i,j+1)\\ &-h\Big[E_x(i,j+1)[B_x(i-1,j+1)+B_x(i,j+1)+B_x(i-1,j)+B_x(i,j)\\ &+E_y(i,j+1)[B_y(i-1,j+1)+B_y(i,j+1)+B_y(i-1,j)+B_y(i,j)]]\Big]\Bigg]\end{aligned} \tag{10}$$

$$\begin{aligned}E_x(i,j+1) =& E_x(i,j)-\frac{dn}{dz}[B_y(i,j)-B_y(i-1,j)]\\ &+2h[\varphi(i,j+1)-\varphi(i,j)][B_x(i,j)+B_x(i-1,j)]\\ &-h\frac{dn}{dz}E_y(i,j)[\varphi(i+1,j+1)+\varphi(i+1,j)-\varphi(i-1,j)-\varphi(i-1,j+1)]\end{aligned} \tag{11}$$

$$\begin{aligned} E_y(i,j+1) =& E_y(i,j) - \frac{dn}{dz}[B_x(i,j) - B_x(i-1,j)] \\ &+ 2h[\varphi(i,j+1) - \varphi(i,j)][B_y(i,j) + B_y(i-1,j)] \\ &- h\frac{dn}{dz}E_x(i,j)[\varphi(i+1,j+1) + \varphi(i+1,j) - \varphi(i-1,j) - \varphi(i-1,j+1)] \end{aligned} \tag{12}$$

$$B_x(i,j+1) = B_x(i,j) + \frac{dn}{dz}[E_y(i+1,j+1) - E_y(i,j+1)] \tag{13}$$

$$B_y(i,j+1) = B_y(i,j) + \frac{dn}{dz}[E_x(i+1,j+1) - E_x(i,j+1)] \tag{14}$$

Lastly, to ensure the continuity of the model, the last points in the electric and magnetic fields are set as equal to the first points. The initial conditions will be shown in the Results section with each case.

3 Results

In this project, three types of wave polarization were focused on: right and left circularly polarized waves, linearly polarized waves, and a linear superposition of right and left-moving linearly polarized waves. All of the cases have the initial conditions for the φ field, which are derived from Equation (15), where $\omega = \sqrt{k^2 + m^2}$. For simplicity, the initial conditions of φ are constant and uniform, but, as will be seen, φ will not remain constant and uniform, which, in turn, will cause the violation of parity.

$$\varphi(z,t) = \cos(kz + \omega t) \tag{15}$$

3.1 Circularly Polarized Waves

The initial conditions of the electric and magnetic fields are derived from the analytical solution of a circularly polarized wave, shown in Equations (17) and (18). Note that $\vec{E} \cdot \vec{B} = 0$, which, in turn, means that $\vec{E}$ and $\vec{B}$ do not have an effect on φ in this case.

$$k = \frac{2\pi}{(Nz-1)dz} \qquad \omega = \sqrt{k^2c^2 + 8hrk} \tag{16}$$

$$\vec{E}(z,t) = \cos(kz + \omega t)\hat{i} - \sin(kz + \omega t)\hat{j} \tag{17}$$

$$\vec{B}(z,t) = -\frac{k}{\sqrt{k^2c^2 + 8hrk}}\sin(kz + \omega t)\hat{i} - \frac{k}{\sqrt{k^2c^2 + 8hrk}}\cos(kz + \omega t)\hat{j} \tag{18}$$

With Equations (15)-(18), the program that generalizes circularly polarized waves was written. In the animation, the velocities of these two waves are different, thus violating parity. Figure 2 illustrates the result of the electric component of the circularly polarized wave.

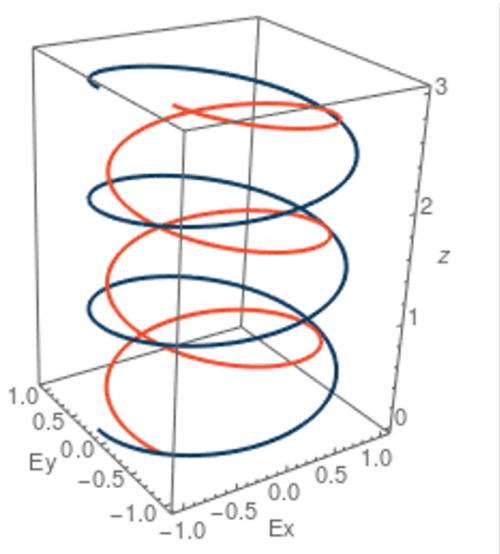

Figure 2: Electric Component of a Circularly Polarized Wave

3.2 Linearly Polarized Waves

The initial conditions of the electric and magnetic fields are derived from the analytical solution of linearly polarized waves, as shown in Equations (19) and (18), and the initial conditions for φ field are the same as in the circularly polarized case (see Equation (15)). Similar to the circularly polarized case, $\vec{E} \cdot \vec{B} = 0$, so the electromagnetic field does not affect φ.

$$\vec{E}(z,t) = \cos(kz + \omega t)\hat{i} \tag{19}$$

$$\vec{B}(z,t) = \cos(kz + \omega t)\hat{j} \tag{20}$$

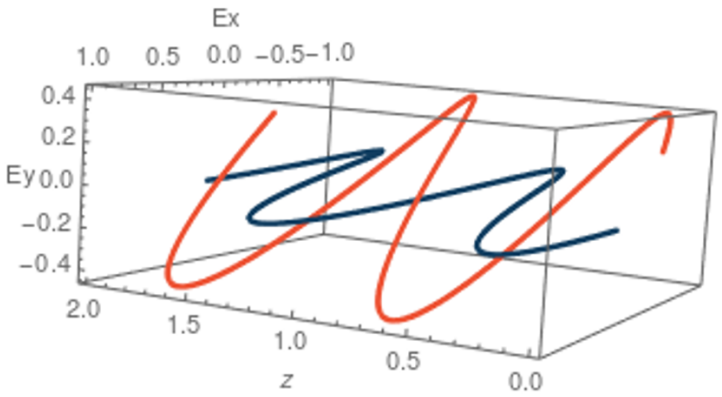

Figure 3: Electric Component of a Linearly Polarized Wave

An image of the animation of these linearly polarized waves in shown in Figure 3. In the animation, the waves rotate at a different rate due to the interaction of axion field, thus demonstrating parity violation.

3.3 Linear Superposition of Right- and Left-moving Linearly Polarized Waves

The final case studied is the linear superposition of right- and left-moving linearly polarized waves. The initial conditions for the electromagnetic field are derived from Equation (21) and (22), and the initial conditions for φ are derived from Equation (15). Unlike the previous two cases, $\vec{E} \cdot \vec{B}$ is no longer constant; as a result, φ is affected by the electromagnetic field. This in turn causes second harmonic generation in the φ field, as shown in Figure 4.

$$\vec{E}(z,t) = \cos(kz + \omega t)\hat{i} + \cos(kz + \omega t)\hat{j} \tag{21}$$

$$\vec{B}(z,t) = \cos(kz - \omega t)\hat{j} + \cos(kz + \omega t)\hat{j} \tag{22}$$

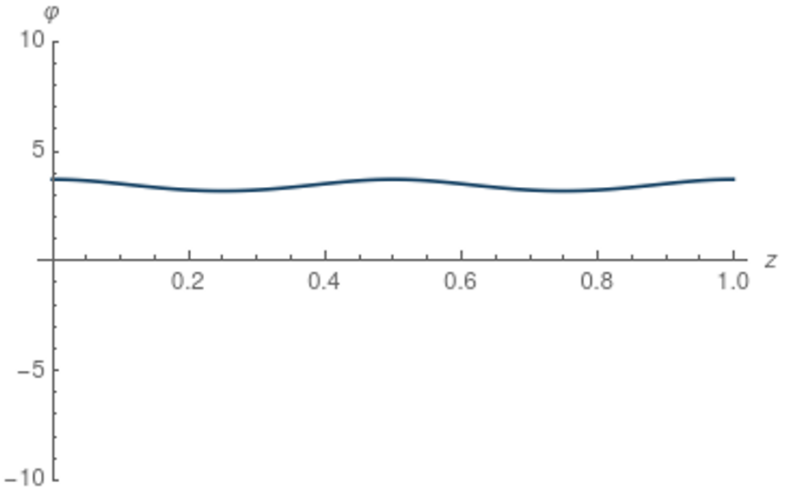

Figure 4: φ field

3.4 Checking the Results

To verify the results, the energy densities of the electromagnetic and φ fields were checked, and the case of the left and right superimposed wave is used as an example. The energy density for this case was constant at first, but varied too much towards the end of the computation to simply be numerical error. Equations (23) and (24) were used to calculate the energy densities of the electromagnetic and φ fields respectively. A graph of the energy densities is shown below in Figure 5) – the black line is the total, the blue is φ, and the orange is the electromagnetic.

$$E(j) = \sum_{i=0}^{Nz} \frac{1}{2}[\tilde{E}_x(i,j)^2 + \tilde{E}_y(i,j)^2 + B_x(i,j)^2 + B_y(i,j)^2] \tag{23}$$

$$E(j) = \sum_{i=0}^{Nz} \frac{1}{2}\Big[[\frac{\varphi(i,j+1) - \varphi(i,j-1)}{2dn}]^2 + [\frac{\varphi(i+1,j) - \varphi(i-1,j)}{2dz}]^2 + m^2\varphi(i,j)^2\Big] \tag{24}$$

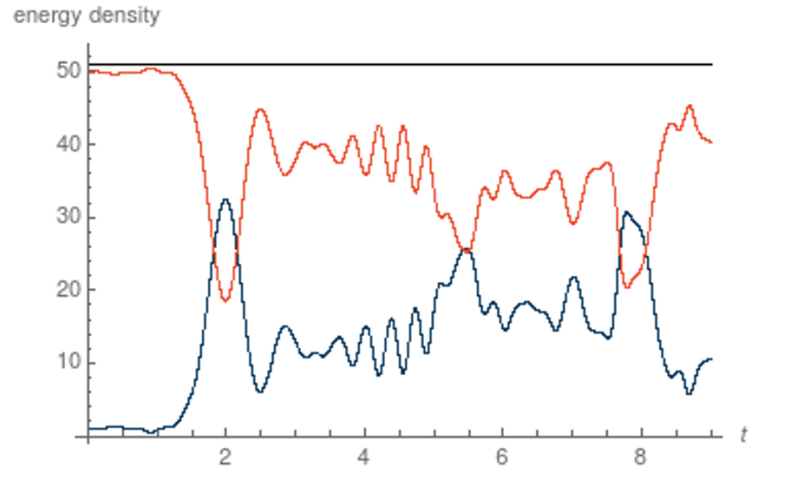

Figure 5: Energy Density of the Electromagnetic and Axion fields

4 Conclusion

In summary, the purpose of this project was to build a computational model of electromagnetic waves that exhibit parity violation. This was done by applying computational theories, such as the staggered lattice model, to the Lagrangian density (Equation (5)) and defining a set of equations for calculating the evolution of the field. The effects of parity violation were studied on three types of wave polarization, and the results were confirmed with conservation of energy.

References

[1] Kane Yee. "Numerical solution of initial boundary value problems involving maxwell's equations in isotropic media". In: *IEEE Transactions on Antennas and Propagation* 14.3 (1966), pp. 302–307. DOI: 10.1109/TAP.1966.1138693.